Int. J. Heat Mass Transfer. Vol. 26, No. 12, pp. 1833-1845, 1983
Printed in Great Britain

0017-9310/83 $3.00 + 0.00
Pergamon Press Ltd.

TURBULENT FLOW HEAT TRANSFER AND FLUID FRICTION IN HELICAL-WIRE-COIL-INSERTED TUBES

R. SETHUMADHAVAN and M. RAJA RAO
Department of Chemical Engineering, Indian Institute of Technology, Bombay 400 076, India

(*Received* 19 *October* 1982)

Abstract—Results are presented from experimental investigations of heat transfer in a 25 mm I.D. copper tube, tightly fitted with helical-wire-coil inserts of varying pitch (p), helix angle (α) and wire diameter (e). A similarity law approach was attempted to interpret the friction and heat transfer results and correlate them in terms of roughness Reynolds number (h^+), momentum transfer roughness function $R(h^+)$ and heat transfer roughness function $G(h^+, Pr)$. The present results are compared with previously published results and a generalized correlation for the G-function has been developed, which is applicable for different types of rough surfaces. An optimization study was made on the basis of maximization of the heat transfer rate and also minimization of pumping power and heat exchanger frontal area to identify the most efficient tube within the matrix of data.

NOMENCLATURE

A	area [m^2]
C	cost [Rs.]
D	tube diameter [m]
e	wire diameter [m]
g	acceleration due to gravity [$m\ s^{-2}$]
h	roughness height [m]
h_i	tube inside heat transfer coefficient [$W\ m^{-2}\ K^{-1}$]
k	thermal conductivity [$W\ m^{-1}\ K^{-1}$]
L	length [m]
p	pitch [m]
ΔP	pressure drop [$N\ m^{-2}$]
Q	heat load [W]
R	radius of tube [m]
T	temperature [°C]
U^*	shear velocity [$m\ s^{-1}$]
V	bulk average velocity [$m\ s^{-1}$]
y	radial distance from the wall [m].

Greek symbols

μ	dynamic viscosity [$N\ s\ m^{-2}$]
γ	kinematic viscosity [$m^2\ s^{-1}$]
ρ	density [$kg\ m^{-3}$]
τ	shear stress [$N\ m^{-2}$]
α	helix angle [°C].

Dimensionless groups

f	friction factor, $2\tau_w g_c/\rho V^2$
$G(h^+, Pr)$	heat transfer roughness function, $\{[(f/2St)-1]/\sqrt{(f/2)}\}+R(h^+)$
h^+	roughness Reynolds number, $(e/D_{eq})\,Re\sqrt{(f/2)}$
Pr	Prandtl number, $C_p\mu/k$
Re	Reynolds number, $DV\rho/\mu$
$R(h^+)$	momentum transfer roughness function, $\sqrt{2/f}+2.5\ln(2e/D_{eq})+3.75$
St	Stanton number, (h_i/GC_p)
u^+	dimensionless velocity, (u/u^*)
y^+	dimensionless radial distance from the wall, (yu^*/γ).

Subscripts

a	augmented tube
b	bulk condition
eq	based on equivalent diameter
i	based on inside diameter
lm	log mean
max	maximum value
0	equivalent smooth tube value
R	ratio
S	smooth tube
W	wall condition.

INTRODUCTION

THE AVAILABILITY of the world's limited material and energy resources and the ever increasing cost of energy over the past few years accelerated the research in the field of conversion of raw materials and reduction in energy usage for a given process. In the heat transfer field, this necessitated the development of compact and more efficient heat transfer equipment. Use of rough surfaces is one of the several enhancement techniques reported by Bergles [1], through which it is possible to achieve a two-fold objective of obtaining the maximum heat transfer rate with a minimum frictional pressure drop. These devices can be employed either to increase the heat transfer rate or to reduce the pumping power or heat transfer area. Considerable work has been reported on internally roughened tubes such as sand-grain roughened tubes [2], internally finned tubes [3, 4], transverse rib-roughened tubes [5–7] and spirally corrugated tubes [8–12], and these are applied with varying degrees of success for a few commercial heat transfer applications. However, very limited work has been published on the thermohydraulic performance of helical-wire-inserted tubes, especially for convective heat transfer applications.

ROUGH SURFACE ANALYSIS

The limited knowledge on the mechanism of flow over rough surfaces hinders the prediction of heat

transfer rates and friction factors by analytical methods because of which the reported equations rely extensively on experimental information. However, the wall similarity law concept, used by Dipprey and Sabersky [2] for sand-grain roughened tubes and later by Webb *et al.* [5] for repeated rib-roughened tubes permits the presentation of experimental results in a most general form taking into account the various parameters involved, inclusive of tube roughness parameters.

The basic similarity law assumptions are the existence of two regions, namely, (a) the inner region, near the wall where the velocity distribution depends exclusively on the local conditions like y, τ_0, μ and h, represented by

$$u^+ (= u/u^*) = F_1\left[\frac{yu^*}{\gamma}\right] = F_1[y^+], \quad (1)$$

and (b) the outer region, the region away from the immediate vicinity of the wall, where the direct effect of viscosity on mean flow is negligible, which can be given by

$$\left(\frac{u_{max}-u}{u^*}\right) = F_2[y/h]. \quad (2)$$

Combination of equations (1) and (2) gives the velocity distribution equation for the turbulent-dominated part of the wall region

$$u^+ = 2.5 \ln (y/h) + R(h^+). \quad (3)$$

Assuming that equation (3) holds good for the entire cross-section of the tube, the friction factor for the turbulent flow inside rough tubes can be given by integration of equation (3). Thus, the friction similarity law for rough surfaces can be represented by

$$R(h^+) = \sqrt{(2/f)} + 2.5 \ln\left(\frac{2h}{D_i}\right) + 3.75. \quad (4)$$

The momentum transfer roughness function $R(h^+)$ is a function of the parameters describing the surface roughness and flow velocity which can be stated for a wire-coil-inserted tube in the form

$$R(h^+) = F[h, p, D_i, \alpha, V, h^+], \quad (5)$$

and (h^+), the roughness Reynolds number is given by

$$h^+ = (h/D_i)\, Re\sqrt{(f/2)}. \quad (6)$$

Nikuradse's [13] pressure drop results, when analysed in terms of $R(h^+)$ and (h^+) showed that for $h^+ > 70$ (this region is termed as a 'fully rough region'), $R(h^+)$ assumed a constant value of 8.48, which was later supported by Dipprey and Sabersky [2] from their study on sand-grain roughened tubes. Later, Webb *et al.* [5] and Ganeshan and Raja Rao [14] used this similarity law approach to correlate the turbulent flow pressure drop results inside repeated rib-roughened tubes and spirally corrugated tubes, respectively. Webb *et al.* also reported that $R(h^+)$ is a function of (p/h) even at higher (h^+) values.

Assuming that the law of wall similarity applies for both velocity and temperature profiles, Dipprey and Sabersky [2] developed a heat transfer similarity law, in analogy with the friction similarity law for flow in a sand-grain roughened tube, and obtained

$$G(h^+, Pr) = \frac{(f/2St-1)}{\sqrt{(f/2)}} + R(h^+). \quad (7)$$

The turbulent heat transfer data for fluids of various Prandtl numbers and tubes of three different sand-grain roughness were correlated well by Dipprey and Sabersky [2] using the function $G(h^+, Pr)$ termed as the heat transfer roughness function, which is ultimately a function of only two variables h^+ and Pr. For a fully rough region ($h^+ > 70$), the following correlation was developed

$$\frac{(f/2St-1)}{\sqrt{(f/2)}} + 8.48 = 5.19\,(Pr)^{0.44}(h^+)^{0.20}. \quad (8)$$

The correlations of Webb *et al.* [5] for heat transfer results obtained in repeated rib-roughened tubes [equation (9)] and of Ganeshan and Raja Rao [14] for multi-start spirally corrugated tubes [equation (10)] showed the negligible effect of tube roughness parameters, expressed as the ratio (p/h) on the G-function

$$\frac{(f/2St-1)}{\sqrt{(f/2)}} + R(h^+) = 4.75(Pr)^{0.57}(h^+)^{0.28}, \quad (9)$$

valid over the range $h^+ > 25$

$$\log [G(h^+, Pr)(Pr)^{-0.55}] = 2.576 - 1.707 \log (h^+) + 0.497(\log h^+)^2 + 0.0103(\log h^+)^3. \quad (10)$$

Though the similarity laws are expected to hold good for any type of roughness geometry, their utility for developing a generalized correlation for a variety of roughness geometries has not yet been fully tested. The objective of this investigation was to generate friction and heat transfer results pertinent to the heating of Newtonian fluids in helical-wire-coil-inserted tubes and correlate the same in terms of $R(h^+)$, $G(h^+, Pr)$ and (h^+) functions and test them with the published results of previous investigators. Further, a parametric evaluation of the tubes, based on three different criteria was attempted to identify the most efficient tube within the matrix of data.

EXPERIMENTAL PROGRAMME

The friction and heat transfer characteristics of eight helical-wire-coil-inserted tubes were determined, for two wire diameters 2.0 and 3.0 mm, and for four helix angles of wire coil, $\alpha = 30°$, 45°, 60° and 75°, corresponding to pitches of 66, 38, 22 and 10 mm, respectively. In addition, one smooth tube was used to standardize the experimental set-up and also to evaluate the increase in the friction factor and tubeside heat transfer coefficient in eight rough tubes, relative to a smooth tube.

Table 1. Characteristic dimensions of the helical-wire-coil-inserted tubes*

Tube	D_{eq} (mm)	p (mm)	e (mm)	α (deg.)	L (mm)
0	25.0	⟵ Smooth tube ⟶			1500
1	22.30	66	2	30	1500
2	21.30	38	2	45	1500
3	19.90	22	2	60	1500
4	16.10	10	2	75	1500
5	21.60	66	3	30	1500
6	20.10	38	3	45	1500
7	18.40	22	3	60	1500
8	12.70	10	3	75	1500

* Water and 50% glycerol were used as working test fluids, flowing in turbulent flow in the tubes over a range of Reynolds number, from 4000 to 100 000.

The characteristic parameters, which define the roughness geometry of the eight helical-wire-coil-inserted tubes are given in Table 1 and a sectional view of one tube is shown in Fig. 1.

A schematic diagram of the experimental set-up is shown in Fig. 2. The actual test section consisted of a 1500 mm long double pipe heat exchanger, the inner tube of which was either the smooth tube or one of the helical-wire-coil-inserted tubes under test. The outer tube of the test rig was a 50 mm I.D. galvanized iron pipe, having openings every 125 mm, displayed radially by 180°, for the passage of thermocouples. Twelve 30-gauge copper–constantan thermocouples were embedded on the heat exchanger tube wall for the measurement of wall temperature. The test section was preceded and followed by smooth tube, or helical-wire-coil-inserted tube calming sections, each with a length of 600 mm, depending on the tube under test.

Each tube was equipped at both the inlet and exit, with three in-plane static pressure wall taps, encompassed by a piezometric ring and in turn each piezometric ring was connected to the limbs of a U-tube manometer. The isothermal pressure drop studies were carried out for turbulent flow of water and 50% glycerol at 30°C. The steady-state pressure drop was measured by means of U-tube manometers using mercury or carbon tetrachloride as manometric liquids, depending upon the magnitude of the flow rate.

Heat transfer studies were carried out for the turbulent flow of water and 50% glycerol inside the inner tube of the heat exchanger using hot water (as the heating medium) flowing at a constant temperature in the annular side of the exchanger. Steady-state flow rates of hot water and test liquid were obtained from calibrated rotameters. The inlet and outlet temperatures of the exchanger fluids and also the metal wall temperatures were obtained from a precision 0.1°C accurate digital temperature indicator.

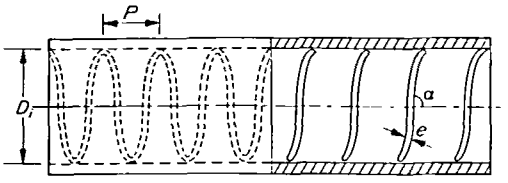

FIG. 1. Characteristic parameters of the helical-wire-coil-inserted tubes. p, pitch of wire coil; e, wire diameter; D_i, inner diameter of tube; and α, helix angle.

RESULTS AND DISCUSSION

Friction factor

The Fanning's friction factor was calculated from

$$f = \frac{D\Delta P g_c}{2\rho V^2 L}. \tag{11}$$

The smooth tube friction factors for the turbulent flow of water and 50% glycerol were well correlated by the Blasius equation

$$f = 0.079(Re)^{-0.25}, \tag{12}$$

with a standard deviation of 2.8%. This served the purpose of standardizing the experimental set-up.

The turbulent flow friction factors in the helical-wire-coil-inserted tubes were found to be higher compared to a smooth tube under the same operating conditions, as seen from Fig. 3. The increase in friction factor ranged from 30% for tubes 1 and 5 (fitted with a wire coil of pitch 66 mm and of wire diameter 2 and 3 mm, respectively), to as high as 220% for tubes 4 and 8 (fitted with wire coils of 2 and 3 mm diameter, respectively, at a closer pitch of 10 mm) compared to a smooth tube. The other tubes produced friction factor enhancements intermediate between 30 and 220%. This order of increase in the friction factor was also earlier reported by Kumar and Judd [15]. Although, the turbulent flow friction factor in these tubes was found to be dependent on the roughness geometry of the tube, it was not independent of Reynolds number even at high flow rates—a trend similar to that observed by Gupta and Raja Rao [9] in spirally corrugated tubes also.

Friction correlation

The results of friction factor in helical-wire-coil-inserted tubes were analysed in terms of the momentum transfer roughness function $R(h^+)$ and roughness Reynolds number (h^+). Figure 4 shows the variation of $R(h^+)$ with (h^+) for the turbulent flow of water and 50% glycerol inside eight helical-wire-coil-inserted tubes. Since the tubes used in the present study are not geometrically similar, a vertical spread in $R(h^+)$ values was observed in Fig. 4. For all the tubes, $R(h^+)$ showed a rising trend with increasing (h^+), which is similar to the trend recently reported by Withers [16] for single-helix corrugated tubes for turbulent flow of water. The $R(h^+)$ values were higher for least rough tubes, namely tubes 1 and 5, and lower for the roughest of all the tubes, namely, tubes 4 and 8. In this study, (h^+) values as high as 2000 were obtained because of the larger wire diameter and closer pitch of helical-wire-winding used.

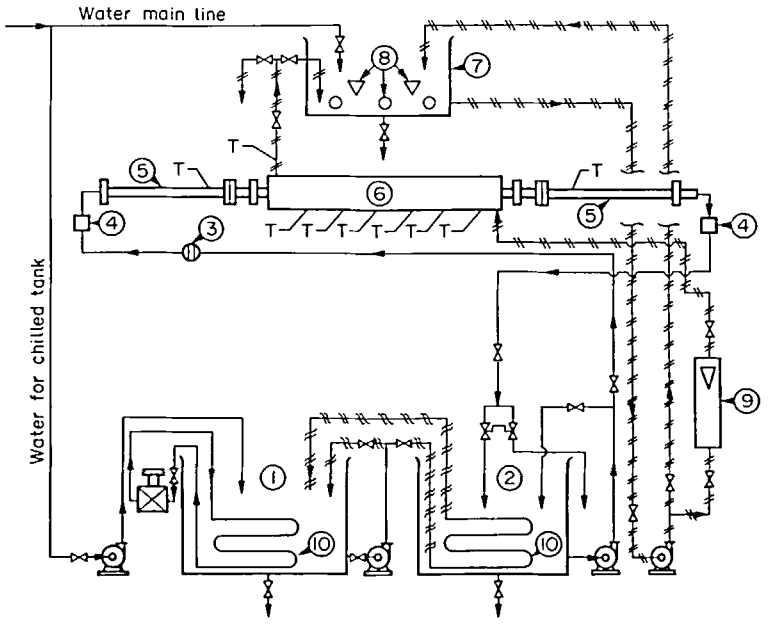

FIG. 2. Schematic diagram of the experimental set-up: (1) chilled water tank; (2) test solution tank; (3) orifice meter; (4) mixing cups; (5) inlet and outlet calming sections; (6) test section; (7) hot water tank; (8) heaters; (9) rotameter; (10) cooling coils; *T*, temperature indicator; *P*, pressure gauge; —, test section line; ⅄—⅄, hot water line; and ⅋—⅋, chilled water line.

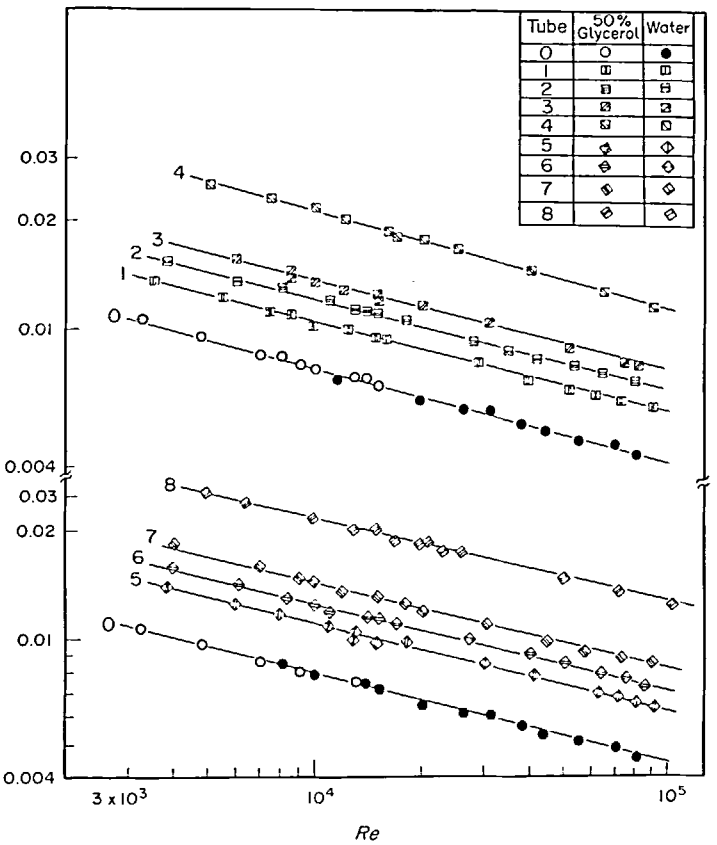

FIG. 3. Variation of f with Re.

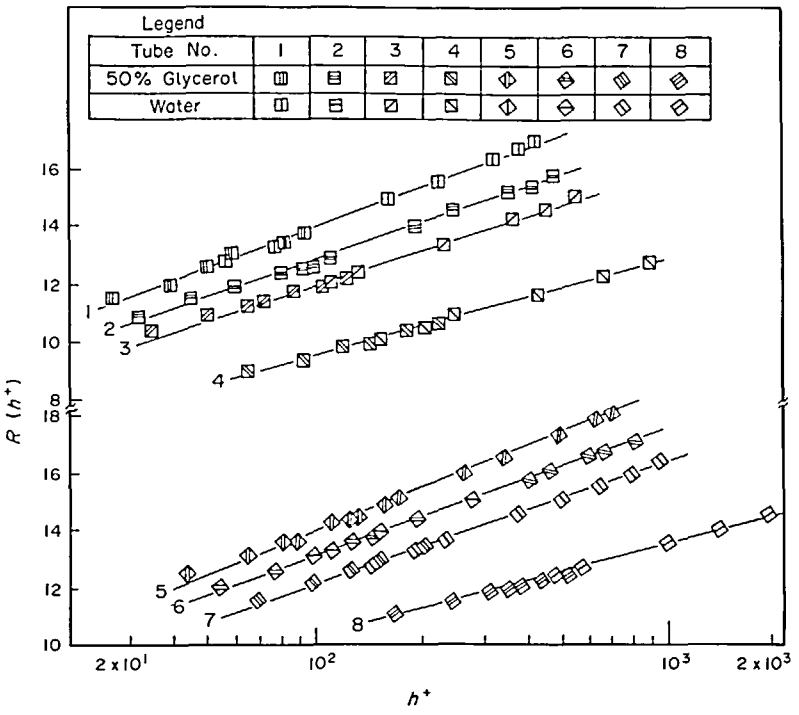

FIG. 4. Variation of $R(h^+)$ with h^+.

Helix angle 'α' was found to be a significant parameter affecting friction in helical-wire-coil-inserted tubes in view of the swirl flow involved. This observation was well supported by the work of Gee and Webb [7] who used helix angle as the correlating parameter between $R(h^+)$ and (h^+).

By cross plotting the present results, $R(h^+)$ was found to be proportional to $(\tan\alpha)^{-0.18}$. The following correlation closely fitted the data points in Fig. 5 within a standard deviation of 6.36, irrespective of wire diameter

$$R(h^+)(\tan\alpha)^{0.18} = 7.0(h^+)^{0.13}. \quad (13)$$

Heat transfer

The tubeside heat transfer coefficient was calculated using

$$Q = h_i A_i (T_w - T_b)_{lm}. \quad (14)$$

The smooth tube heat transfer data were found to agree within $\pm 5\%$ with the Sieder–Tate heat transfer equation for turbulent flow

$$\frac{h_i D_i}{k} = 0.027[Re]^{0.8}[Pr]^{0.33}[\mu/\mu_w]^{0.14}. \quad (15)$$

The tubeside heat transfer coefficients for the

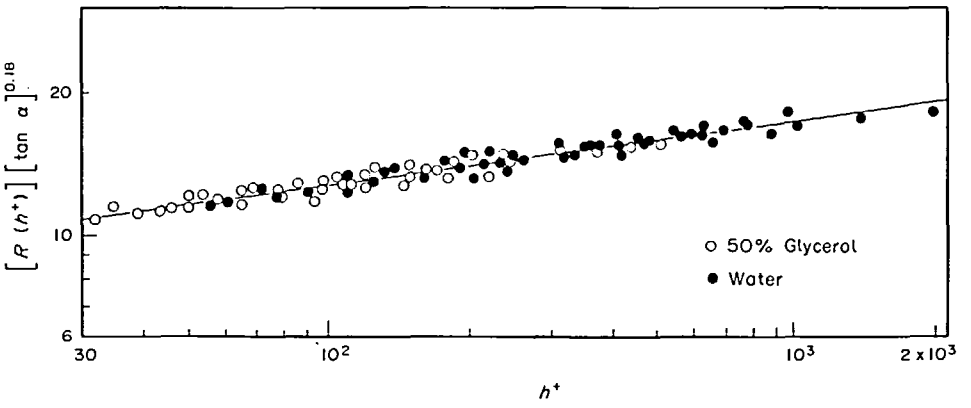

FIG. 5. Variation of $[R(h^+)][\tan\alpha]^{0.18}$ with roughness Reynolds number $[h^+]$ for the flow of water and 50% glycerol in helical-wire-coil-inserted tubes—final correlation.

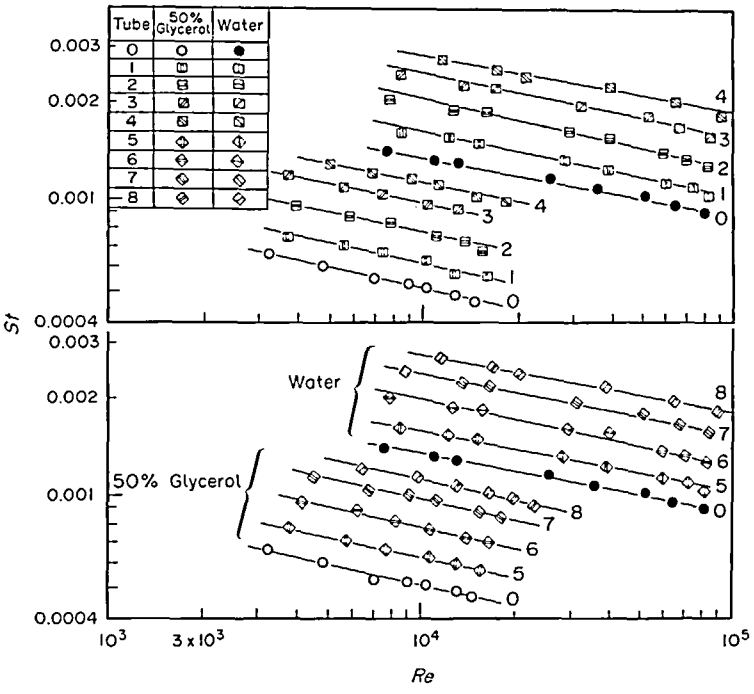

FIG. 6. Variation of *St* with *Re*.

turbulent flow of water and 50% glycerol in one smooth tube and eight helical-wire-coil-inserted tubes were analysed in terms of *St*–*Re* relationships and Fig. 6 shows the variation of *St* with *Re* for all the tubes.

The Stanton numbers for the heating of both the test fluids in these tubes were predominantly higher compared to the smooth tube, at the same Reynolds number. The roughest tubes 4 and 8 of the present work produced a maximum improvement in Stanton number of the order of 150%, whereas tubes 1 and 5

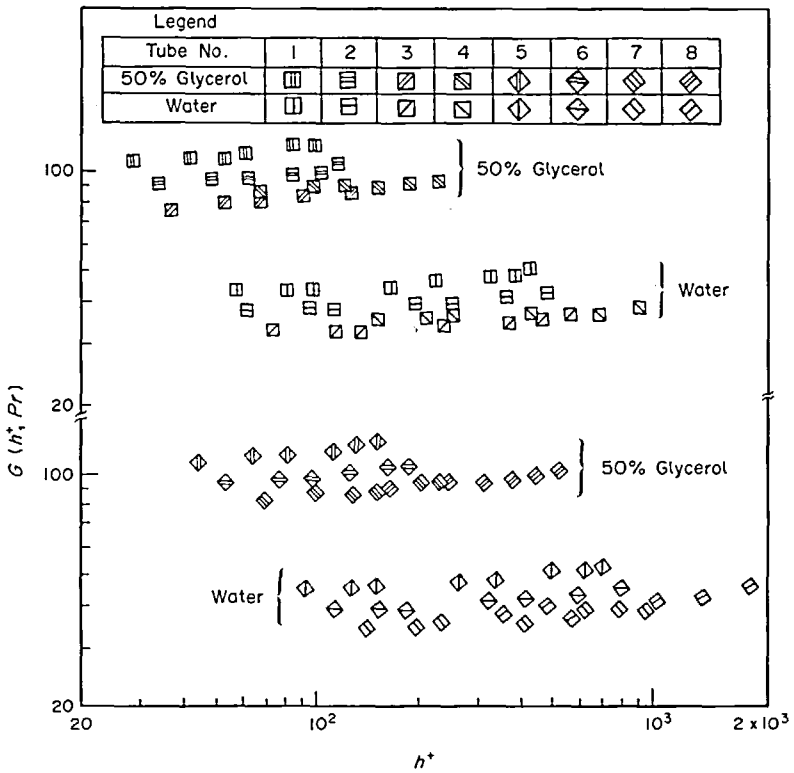

FIG. 7. Variation of $G(h^+, Pr)$ with h^+.

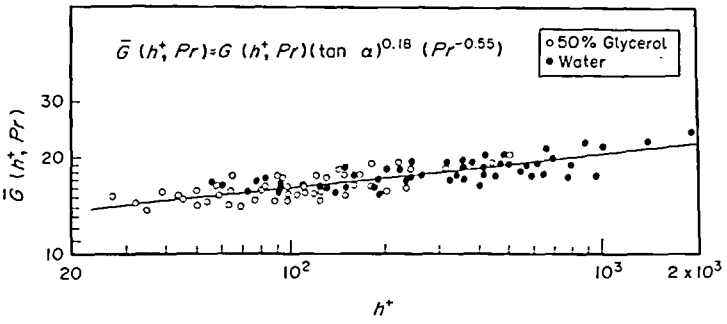

FIG. 8. Variation of $\bar{G}(h^+, Pr)$ with h^+.

(least rough coil-inserted tubes) yielded an improvement of 25% only in the Stanton number, compared to the smooth tube.

Heat transfer correlation

Variation of the heat transfer roughness function $G(h^+, Pr)$ computed from equation (7) is plotted against roughness Reynolds number (h^+) in Fig. 7, for water and 50% glycerol flowing in eight helical-wire-coil-inserted tubes.

The G-function for each tube increased slightly with an increase in (h^+) and further its value is different for each tube, although the difference is not very pronounced. This clearly shows that the G-function is a weak function of h^+ and the helical-wire-coil geometry. However, $G(h^+, Pr)$ is a strong function of the fluid Prandtl number.

Gee and Webb [7] reported that the G-function was influenced by the helix angle of the insert and further they found that the air data of Nunner [17] and Han *et al.* [18] could also be correlated in the same way. The agreement was found to be excellent. In the present study, the tangent of the helix angle $(\tan\alpha)$, which adequately defined the helical-wire-coil geometry was used for correlating $G(h^+, Pr)$ with (h^+), apart from the fluid Prandtl number.

Cross-plotting of the G-function against $(\tan\alpha)$ at selected (h^+) values showed that $G(h^+, Pr)$ varied with $(\tan\alpha)^{-0.18}$. The effect of the wire diameter of the coil insert on the heat transfer rate was found to be negligible in the present study, thus confirming the previous findings of Kumar and Judd [15].

The influence of Prandtl number on the G-function was evaluated by the treatment of heat transfer results of the two test liquids $(5.2 < Pr < 32)$ used and $G(h^+, Pr)$ was found to vary directly with $Pr^{0.55}$. This agreed well with the function $Pr^{0.55}$ obtained by Ganeshan and Raja Rao [14] and compared well with $Pr^{0.57}$ reported by Webb *et al.* [5] for repeated rib-roughened tubes. Figure 8 shows the variation of $G(h^+, Pr)(\tan\alpha)^{0.18}(Pr^{-0.55})$ with (h^+) for the heating of the test liquids in eight helical-wire-coil-inserted tubes and the final correlation was obtained as

$$G(h^+, Pr)(\tan\alpha)^{0.18}(Pr^{-0.55}) = 8.6(h^+)^{0.13}. \quad (16)$$

Equation (16) predicted the results of the present work and also the results of Carnavos [4] for water inside helical-finned-tubes and of Kumar and Judd [15] for water in tubes fitted with turbulence promoters. This comparison is shown in Fig. 9.

PERFORMANCE EVALUATION

In technically evaluating the performance of eight helical-wire-coil-inserted tubes, criteria 3–5, based on the objectives of (a) maximizing heat transfer rate, (b) minimizing pumping power and (c) minimizing exchanger size, as suggested by Bergles *et al.* [19] were used. The performance ratios were not only evaluated as the ratio (h_{ia}/h_{is}) but also as $[U_a/U_s]$ in view of the fact

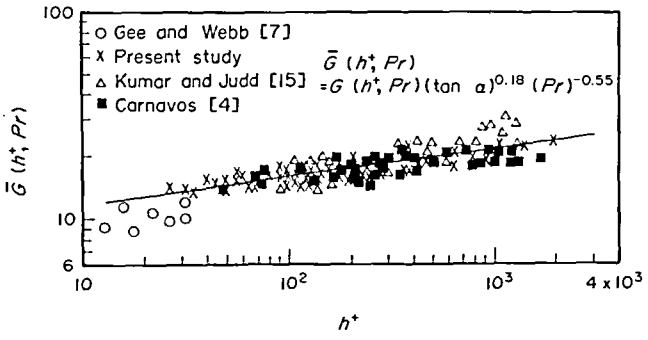

FIG. 9. Comparison of the present correlation with the results of other workers.

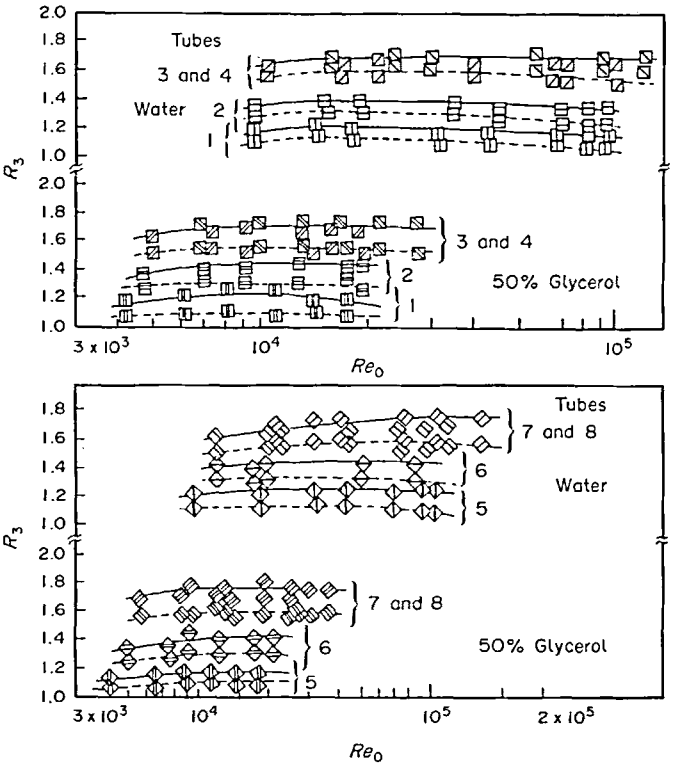

FIG. 10. Variation of R_3 with Re_0: ——, $r = 0$; ----, r = finite value.

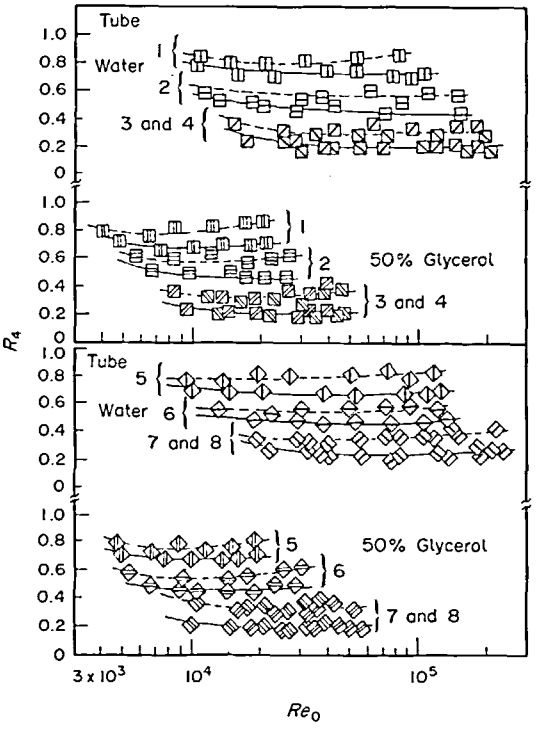

FIG. 11. Variation of R_4 with Re_0: ——, $r = 0$; ----, r = finite value.

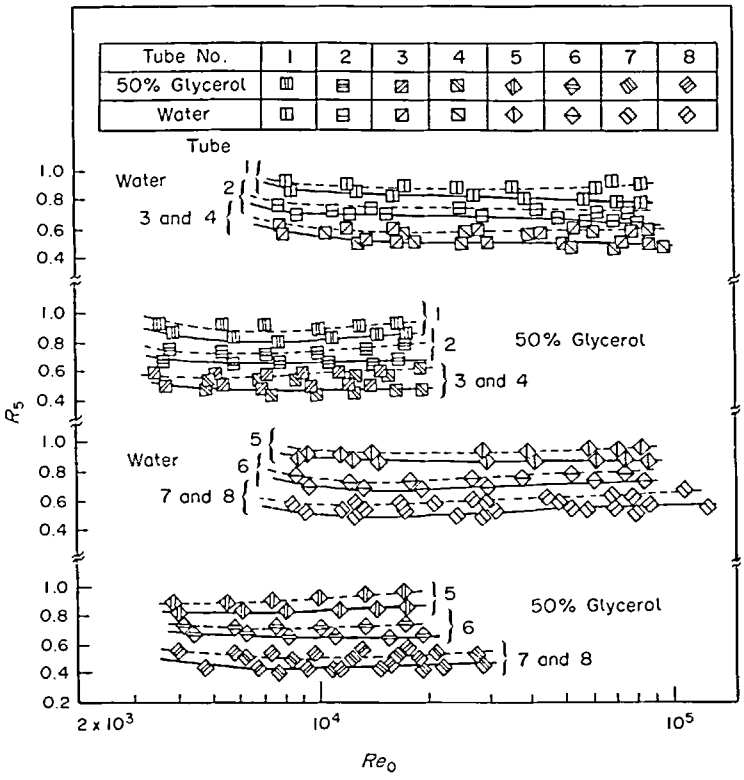

FIG. 12. Variation of R_5 with Re_0: ——, $r = 0$; ----, r = finite value.

that 'r' (the ratio of combined outside film and metal wall resistance to the inside film resistance) is not zero, but ranged from 0.3 to 2.5 for the overall range of Reynolds number, 4000–100 000, studied.

Criterion 3

Figure 10 shows the variation of performance ratio R_3 with equivalent smooth tube Reynolds number Re_0, for all the eight rough tubes studied. The enhancement in the heat transfer rate varied from a minimum of 15% (in tubes 1 and 5) to a maximum of 85% (in tubes 3, 4, 7 and 8) based on the ratio of individual heat transfer coefficients, namely, (h_{ia}/h_{is}). This is comparable to the augmentation of 75% obtained by Carnavos [4] for the heating of water in internal helical-finned-tubes. However, when R_3 is evaluated as U_a/U_0 and plotted against Re_0 in Fig. 9 as dotted curves, the performance ratio showed a slight reduction. This behaviour was expected, especially at higher Reynolds numbers where $r(= h_i/h_0) \neq 0$, since h_i is either comparable to or slightly higher than the tube outside heat transfer coefficient (h_0). Thus the R_3 value ($= U_a/U_0$) ranged from 1.1 to 1.6 only for the eight tubes used in the present study. The best operating Re_0 was 20 000–50 000 for water and 8000–15 000 for 50% glycerol.

Criterion 4

This criterion aims at a reduction in the pumping power for equal heat duty and surface area (i.e. $Q/Q_s = A/A_s = 1$). The performance ratio $R_4(= P_a/P_0)$ is plotted against Re_0 in Fig. 11.

Based on h_i, the reduction in pumping power varied from 30% for least rough tubes (tubes 1 and 5) to 80 for the roughest tubes (tubes 3, 4, 7 and 8). However, when the ratio R_4 was evaluated on the basis of the overall heat transfer coefficients, a maximum reduction of pumping power of 70% only was observed for tubes 3, 4, 7 and 8. In this case also, all the tubes seem to perform well in the Re_0 range, from 20 000 to 50 000 for water and 9000 to 15 000 for 50% glycerol.

Criterion 5

The performance ratio R_5 (based on both h_i and U) is shown as a function of Re_0 in Fig. 12 for all the eight helical-wire-inserted tubes.

The replacement of a smooth tube by tubes 3, 4, 7 and 8 produced a heat transfer area reduction of 50–60% which compared well with a reduction of 45% observed by Marto *et al.* [20] by using roped tubes instead of a smooth tube.

However, the maximum reduction in heat exchanger frontal area obtained was only 50%, using tubes 3, 4, 7 and 8, when R_5 was based on U (that is $-\gamma$ is finite). All the eight tubes performed well in the Re_0 range of 15 000–40 000 for water and 7000–12 000 for 50% glycerol.

However, in evaluating the performance of these tubes, the effects of fouling, cost factor, etc. are not taken

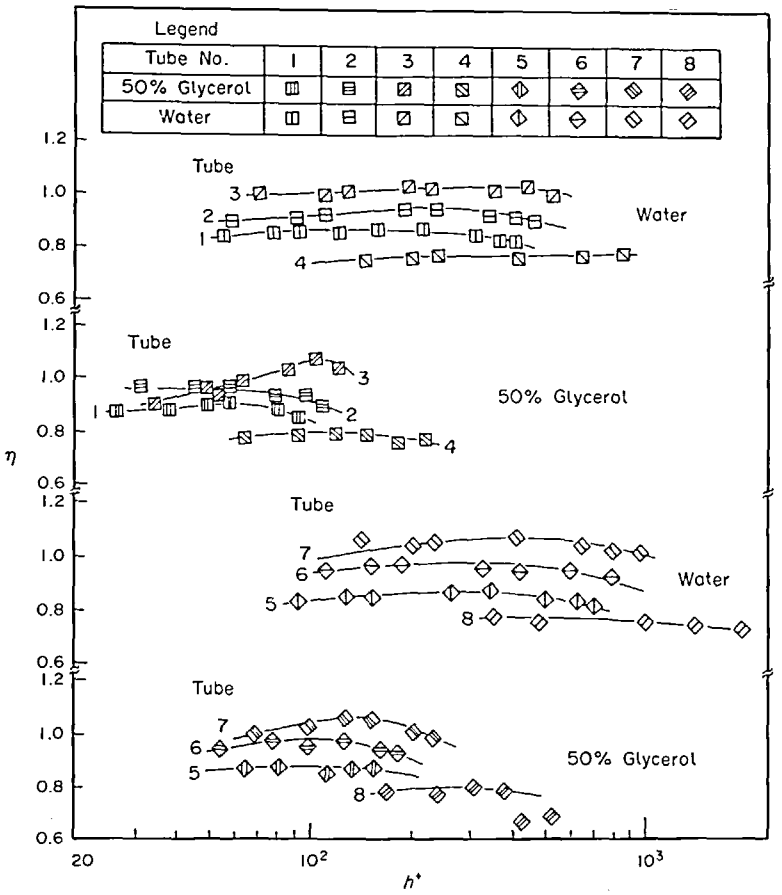

FIG. 13. Variation of η with h^+.

into consideration, which might, however, influence the final selection of the tubes for use in heat exchangers.

TUBE EFFICIENCY INDEX

The efficiency index 'η' of eight helical-wire-coil-inserted tubes was evaluated as

$$\eta = \left(\frac{St_a/St_s}{f_a/f_s}\right), \tag{17}$$

as suggested by Gee and Webb [7].

From Fig. 13, where 'η' is plotted against h^+, it can be seen that 'η' slowly increased with increasing (h^+), reached a maximum value and then started decreasing with a further increase in (h^+). The overall variation of 'η' with h^+ with any of the eight tubes was, however, very small.

In order to establish the effect of helix angle α on the tube efficiency index 'η', η is plotted against 'α' in Fig. 14 for two selected values of h^+, and the results showed that optimum helix angle lies in the vicinity of 50°–60° for both the fluids, namely, water and 50% glycerol.

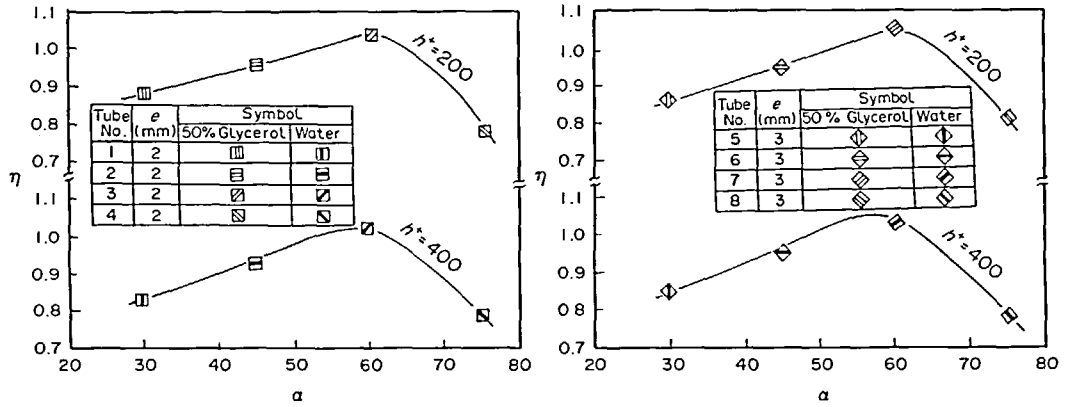

FIG. 14. Variation of efficiency index (η) with helix angle (α) for the heating of water and 50% glycerol in helical-wire-coil-inserted tubes.

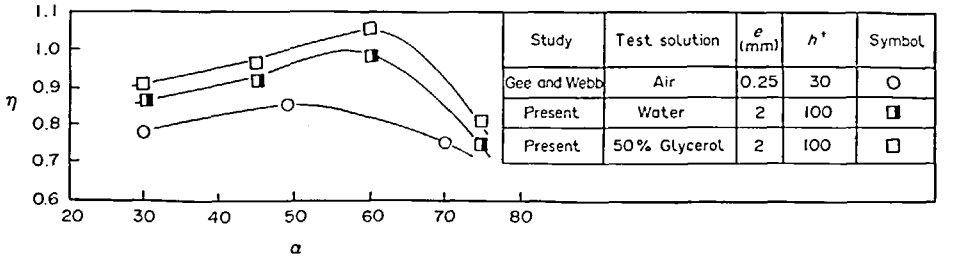

Study	Test solution	e (mm)	h⁺	Symbol
Gee and Webb	Air	0.25	30	○
Present	Water	2	100	◧
Present	50% Glycerol	2	100	□

FIG. 15. Comparison of the results η vs α of the present work with those of other workers.

The present results and those of Gee and Webb [7] were compared in Fig. 15. According to Gee and Webb [7], a maximum efficiency index of 0.85 was observed at a helix angle of 49° for a (h^+) value of 30, for the heating of air ($Pr = 0.71$). However, in the present study the optimum angle corresponding to a maximum value of 1.05 for the efficiency index seemed to lie around 55° for water ($Pr = 5.2$) and 60° for 50% glycerol ($Pr = 32$). It is clear from Fig. 15, that optimum helix angle increases slightly with an increase in Prandtl number of the test fluid used. This behaviour suggests that higher helix angle might be preferable for the heating of higher Prandtl number fluids.

COST ANALYSIS

Since, the material of the helical wire insert adds to the cost of the smooth tubes, an attempt was made to compute the cost of the enhanced tubes with the insert and to identify the tube which performs superior to other tubes, on the basis of cost ratio also. The cost ratio C_R is calculated as

$$C_R = \left(\frac{C_a}{C_s}\right), \qquad (18)$$

where C_a is the cost of the augmented tube (cost of the smooth tube plus cost of the wire added), and C_s is the cost of the smooth tube. Figure 16 shows the variation of performance ratios R_3, R_4 and R_5 as a function of C_R. Though tubes 3, 4, 7 and 8 produced the same performance ratios, tube 3 has accomplished it at the least cost ratio C_R(= 1.15) and hence tube 3 is established as the most favoured tube in the present work.

CONCLUDING REMARKS

The results of the present study indicate conclusively that:

(1) The preferred helix angle of the wire-coil promoter is in the vicinity of 50°–55° for convective heat transfer to water and around 60° for 50% glycerol.

(2) Evaluation of thermal performance of the tubes based on criteria 3–5 and also cost factor considerations showed that tube 3 is the most efficient of all the eight tubes.

(3) A correlation for $G(h^+, Pr)$ is proposed, based on the results of the present work and those of previous investigators on tubes of different roughness geometries.

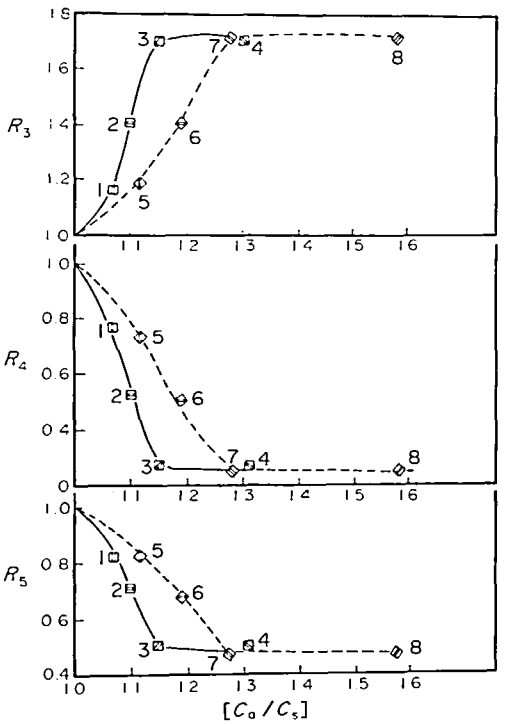

FIG. 16. Variation of performance ratios with cost ratio in helical-wire-coil-inserted tubes.

REFERENCES

1. A. E. Bergles, Enhancement of heat transfer, *Proc. 6th Int. Heat Transfer Conf.*, Vol. 6, p. 89. Toronto (1978).
2. D. F. Dipprey and R. H. Sabersky, Heat and momentum transfer in smooth and rough tubes, *Int. J. Heat Mass Transfer* 6, 329 (1963).
3. A. P. Watkinson, D. L. Miletti and P. Tarassoft, Turbulent heat transfer and pressure drop in internally finned tubes, *A.I.Ch.E. Symp. Ser.* 131 (169), 94–103 (1973).
4. T. C. Carnavos, Heat transfer performance of internally finned tubes in turbulent flow, Symp. on Advances in Enhanced Heat Transfer, pp. 61–67, 18th National Heat Transfer Conference, San Diego (1979).
5. B. L. Webb, E. R. G. Eckert and R. J. Goldstein, Heat transfer and friction in tubes with repeated rib roughness, *Int. J. Heat Mass Transfer* 14, 601–617 (1971).
6. M. Dalla Donne and E. Meyer, Turbulent convective heat

transfer from surfaces with two-dimensional rectangular ribs, *Int. J. Heat Mass Transfer* **20**, 584–620 (1977).
7. D. L. Gee and R. L. Webb, Forced convection heat transfer in helically rib-roughened tubes, *Int. J. Heat Mass Transfer* **23**, 1127–1136 (1980).
8. J. W. Smith, R. A. Gowen and M. E. Charles, Turbulent heat transfer and temperature profiles in a rifled pipe, *Chem. Engng Sci.* **23**, 751–758 (1968).
9. R. K. Gupta and M. Raja Rao, Heat transfer and friction characteristics of Newtonian and power law type of non-Newtonian fluids in smooth and spirally corrugated tubes, Symp. on Enhanced Heat Transfer, pp. 103–113, 18th National Heat Transfer Conference, San Diego (1979).
10. G. J. Kidd, Jr., Heat transfer and pressure drop characteristics of gas flow inside spirally corrugated tubes, *Am. Soc. Mech. Engrs*, Series C, *J. Heat Transfer* **92**, 513–519 (1970).
11. J. G. Withers, E. H. Young and W. B. Lampert, Heat transfer characteristics of corrugated tubes, *Chem. Engng Prog. Symp. Ser.* **174** (74), 15–24 (1978).
12. M. H. Mehta and M. Raja Rao, Heat transfer and frictional characteristics of spirally enhanced tubes for horizontal condensers, Symp. on Enhanced Heat Transfer, pp. 11–21, 18th National Heat Transfer Conference, San Diego (1979).
13. J. Nikuradse, Gestz map igkeit der turbulenten storomung in glatten Rohren, *Forschungscheft* 356 (1932).
14. S. Ganeshan and M. Raja Rao, Studies on thermohydraulics of single- and multi-start spirally corrugated tubes for water and time independent power law fluids, *Int. J. Heat Mass Transfer* **25**, 1013–1022 (1982).
15. P. Kumar and R. L. Judd, Heat transfer with coiled wire turbulence promoters, *Can. J. Chem. Engng* **48**, 378–383 (1970).
16. J. G. Withers, Tube side heat transfer and pressure drop for tubes having helical internal ridging with turbulent/transitional flow of single-phase fluid–part I single-helix ridging, *Heat Transfer Engng* **2**, 48–58 (1980).
17. W. Nunner, Heat Transfer and pressure drop in rough pipes, *VDI Forschft* **22**, 4558 (1959).
18. J. C. Han, L. R. Glicksman and L. M. Rohsenow, An investigation of heat transfer and friction of rib roughened surfaces, *Int. J. Heat Mass Transfer* **21**, 1143–1156 (1978).
19. A. E. Bergles, A. R. Blumenkrantz and J. Taburek, Performance evaluation criteria for enhanced heat transfer surfaces, *Proc. 5th Int. Heat Transfer Conf.*, Vol. II, Paper FC 6-3 Tokyo (1974).
20. P. J. Marto, D. J. Reilly and J. H. Fenner, An experimental comparison of enhanced heat transfer condenser tubing, Symp. on Enhanced Heat Transfer, pp. 1–9, 18th National Heat Transfer Conference, San Diego (1979).

TRANSFERT THERMIQUE TURBULENT ET FROTTEMENT POUR DES FILS HELICOÏDAUX INSERES DANS DES TUBES

Résumé—On présente des résultats expérimentaux de transfert de chaleur dans un tube en cuivre de diamètre intérieur 25 mm, muni d'un serpentin de fil inséré avec un pas (p), un angle d'hélice (α) et un diamètre de fil (e). Une loi de similitude est fournie pour interpréter le frottement et le transfert thermique et les formules en fonction du numbre de Reynolds de rugosité (h^+), du transfert de quantité de mouvement $R(h^+)$ et du transfert thermique $G(h^+, Pr)$. Ces résultats obtenus sont comparés avec des résultats déjà publiés et une formule générale pour la fonction G est développée et elle est applicable pour différents type de surfaces rugueuses. Une étude d'optimisation est faite sur la base de la maximisation du transfert thermique et de la réduction de la puissance de pompage et de l'aire frontale de l'échangeur de chaleur, afin d'identifier le tube le plus efficace dans l'ensemble des données.

TURBULENTER WÄRMEÜBERGANG UND DRUCKABFALL IN ROHREN MIT EINGESETZTEN SPIRALFÖRMIGEN DRAHTWENDELN

Zusammenfassung—Es werden die Ergebnisse experimenteller Untersuchungen des Wärmeübergangs in einem Kupferrohr von 25 mm Durchmesser, in dem spiralförmige Drahtwendeln eng anliegend eingebracht wurden, mitgeteilt. Ganghöhe (p), Steigungswinkel (α) und der Drahtdurchmesser (e) wurden variiert. Es wurde versucht, die Ergebnisse für Wärmeübertragung und Druckverlust entsprechend den Ähnlichkeitsgesetzen zu deuten und sie in Abhängigkeit von Begriffen wie der Rauhigkeits-Reynolds-Zahl (h^+), der Rauhigkeits-Impulsübertragungs-Funktion $R(h^+)$ und der Rauhigkeits-Wärmeübertragungs-Funktion $G(h, Pr)$ darzustellen. Die vorliegenden Ergebnisse werden mit früher veröffentlichten verglichen und eine allgemeine Beziehung für die G-Funktion entwickelt, die auf verschiedene Arten von rauhen Oberflächen anwendbar ist. Um das günstigste Rohr innerhalb der ermittelten Daten zu identifizieren, wurde eine Optimierungsuntersuchung gemacht, deren Grundlage die Maximierung des Wärmeübergangs sowie die Minimierung der Pumpenleistung und der Wärmeaustauscherstirnfläche ist.

ТЕПЛОПЕРЕНОС ПРИ ТУРБУЛЕНТНОМ ТЕЧЕНИИ И ТРЕНИЕ ЖИДКОСТИ В ТРУБАХ С ПРОВОЛОЧНЫМИ СПИРАЛЬНЫМИ ВСТАВКАМИ

Аннотация—Представлены результаты экспериментальных исследований теплопереноса в медной трубе, имеющей внутренний диаметр 25 мм, в которую вплотную вмонтированы проволочные спиральные вставки с разными шагами (p), углами наклона витков (α) и диаметрами проволоки (e). Предпринята попытка на основе автомодельного анализа объяснить результаты по трению и теплопереносу и обобщить их с помощью числа Рейнольдса для шероховатой поверхности (h^+), функции переноса количества движения на шероховатой поверхности $R(h^+)$ и функции переноса от шероховатой поверхности $G(h^+, Pr)$. Проведено сравнение полученных результатов с ранее опубликованными данными и предложено обобщенное соотношение для G-функции, которое можно использовать для различных типов шероховатых поверхностей. Используя матрицу экспериментальных данных, выполнен анализ оптимизации рассматриваемого теплообменного устройства по максимуму теплового потока, минимуму мощности, необходимой для прокачки жидкости, и минимуму фронтальной площади теплообменника.